ELSEVIER

Journal of Organometallic Chemistry 498 (1995) 15–24

Journal of Organometallic Chemistry

Formation and X-ray structure of the μ-alkylidene complex $Fe_2(CO)_6(\mu-\eta^3, \eta^3\text{-}C(CH{=}CHPh)_2)$ upon deoxygenation of $Fe_2(CO)_8(\mu-\eta^2, \eta^2\text{-}C(O)(CH{=}CHPh)_2)$ with methyl lithium ☆

Sylvain Bernès [a], Rubén A. Toscano [a], Andrés C. Cano [a], Olivia García Mellado [a],
Cecilio Alvarez-Toledano [a,*], Henri Rudler [b,*], Jean-Claude Daran [c]

[a] *Instituto de Química, Circuito Exterior, Ciudad Universitaria, Coyoacán 04510, Mexico*
[b] *Laboratoire de Chimie Organique, URA CNRS 408, Université Pierre et Marie Curie, 4, Place Jussieu, 75252 Paris Cedex 05, France*
[c] *Laboratoire de Chimie de Coordination, UPR CNRS 8241, Université Paul Sabatier, 205, Route de Narbonne, 31077 Toulouse Cedex, France*

Received 10 October 1994

Abstract

Di-iron nonacarbonyl reacts with dibenzylideneacetone (**5**) to produce, depending on the reaction conditions, either a mixture of the three complexes $Fe(CO)_4[\eta^2(CO)(CH{=}CHPh)_2]$ (**6**), $Fe_2(CO)_8[\eta^2, \eta^2(CO)(CH{=}CHPh)_2]$ (**7**), and $Fe(CO)_3[\eta^4(CO)(CH{=}CHPh)_2]$ (**8**), or solely complex **7** in which the ligand is bound in a η^2, $\mu-\eta^2$, η^2, or η^4 fashion. All three complexes have been fully characterized by X-ray crystallography. Crystal data for complex **6**: $C_{21}H_{14}FeO_5$, monoclinic, space group $P2_1/n$, $a = 6.326(2)$ Å, $b = 14.567(2)$ Å, $c = 20.504(2)$ Å, $\beta = 96.91(2)°$, $U = 1875(4)$ Å^3, $D_c = 1.42$ g cm^{-3}, $Z = 4$. For complex **7**: $C_{25}H_{14}Fe_2O_9$, triclinic, space group $P\bar{1}$, $a = 9.677(5)$ Å, $b = 10.635(5)$ Å, $c = 13.471(6)$ Å, $\alpha = 104.24(3)°$, $\beta = 105.46(4)°$, $\gamma = 104.75(4)°$, $U = 1216.7(8)$ Å^3, $D_c = 1.56$ g cm^{-3}, $Z = 2$. For complex **8**: $C_{20}H_{14}FeO_4$, orthorhombic, space group $Pbca$, $a = 13.397(2)$ Å, $b = 10.041(3)$ Å, $c = 26.579(2)$ Å, $U = 3575.1(8)$ Å^3, $D_c = 1.39$ g cm^{-3}, $Z = 8$. Upon reaction with MeLi under an atmosphere of CO, all of the three complexes each gave a mixture of the expected η^4-ketene complex $Fe(CO)_4(\eta^4\text{-}PhCH{=}CH(C{=}C{=}O)CH{=}CHPh)$ (**9**) as the result of a deoxygenation–carbonylation reaction, and the new μ-alkylidene complex $Fe_2(CO)_6(\mu-\eta^3, \eta^3\text{-}C(CH{=}CHPh)_2)$ (**10**) as the result of a deoxygenation reaction of the starting complex followed by the trapping of the intermediate alkylidene complex by $Fe(CO)_3$. Complex **10**, $C_{23}H_{14}Fe_2O_6$, has been fully characterized by X-ray crystallography and shown to be orthorhombic, space group $Pbcn$, $a = 17.155(4)$ Å, $b = 7.842(2)$ Å, $c = 15.857(2)$ Å, $U = 2133.2(5)$ Å^3, $D_c = 1.55$ g cm^{-3}, $Z = 4$.

Keywords: Iron; Ketene; Alkylidene complexes; Dibenzylideneacetone

1. Introduction

Recent work by Thomas et al. [1] demonstrated the role that Fe(0) η^4-vinyl ketone complexes can play in organometallic chemistry as well as in organic chemistry. Especially important was the observation of the formation of vinyl ketene complexes from the attack of an organolithium compound on a carbonyl ligand of the metal. The investigation of the mechanism for this transformation suggests the formation of transient vinyl-carbene complexes (Scheme 1, **1** → **3**) which undergo an insertion of CO (**3** → **4**).

However, direct evidence for the formation of an unstable carbene complex such as compound **3** has not been established, although organic coupling products of the presumed carbene complexes have been detected [1,2] and heteroatom-substituted carbene complexes of iron have been found to undergo easy CO-insertion reactions [3,4] leading to coordinated ketene complexes.

During our studies of the interaction of amines, especially tertiary amines, with ketene complexes of chromium [5,6] and of iron [2], we attempted the synthesis of ketene complexes derived from functionalized vinyl ketones, among which were divinyl ketones.

☆ Contribution No. 1257 of the Instituto de Química, UNAM.

* Corresponding authors.

SSDI 0022-328X(95)05457-X

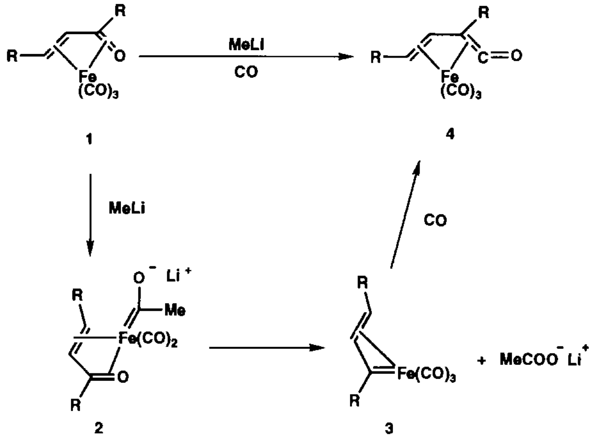

Scheme 1.

Here we present evidence that suggests the formation of an intermediate alkylidene complex.

2. Results and discussion

2.1. Synthesis of the vinyl-ketone complexes

When dibenzylideneacetone (**5**) was treated in anhydrous ether, at room temperature, with an excess of $Fe_2(CO)_9$, the complex $Fe_2(CO)_8$ [η^2, η^2(CO)-(CH=CHPh)$_2$] (**7**) precipitated as a yellow powder, in a 22% yield. Silica-gel chromatography of the residue obtained upon evaporation of the solvent gave a further crop of complex **7** [7] (6%) together with complexes $Fe(CO)_4$[η^2(CO)(CH=CHPh)$_2$] (**6**) (8.5%) and $Fe(CO)_3$[η^4(CO)(CH=CHPh)$_2$] (**8**) (18%). The structures of these complexes were assigned spectroscopically and confirmed by X-ray diffraction (Scheme 2).

The ^{1}H NMR spectrum of complex **6** disclosed doublets centred at δ 7.77 and 7.08 ppm (d, $J = 16$ Hz) for the vinylic protons of the free carbon–carbon double bond, and at δ 4.59 and 5.33 ppm (d, $J = 11.4$ Hz) for those of the coordinated double bond. The upfield shift observed for the vinylic protons of the coordinated double bond is similar to those reported in tetracarbonyl (cinnamaldehyde) iron(0) [8] and tetracarbonyl (chalcone) iron(0) [9], suggesting that in complex **6**, an $Fe(CO)_4$ fragment is bound in an η^2 fashion to the ligand. Moreover, the carbons of the free and coordinated double bonds gave signals at respectively δ 141.9 and 125.7 ppm, and at 53.3 and 57.7 ppm as compared with the shift observed for the free ketone, at δ 142.9 and 125.5 ppm.

The ORTEP view of complex **6** appears in Fig. 1 whereas the bond distances (Å) and the bond angles (deg) are listed in Table 1. This shows the η^2 coordination of the ketone to $Fe(CO)_4$, with a lengthening of the coordinated double bond C(2)–C(3), 1.409(3) Å, compared with a C(4)–C(5) free double bond length of 1.313(4) Å. No difference in the bond distance for C(2)–C(1) and C(1)–C(4) is, however, observed.

The IR spectrum of the second complex (**7**) showed four ν (MCO) bands typical of (olefin)$Fe(CO)_4$ sys-

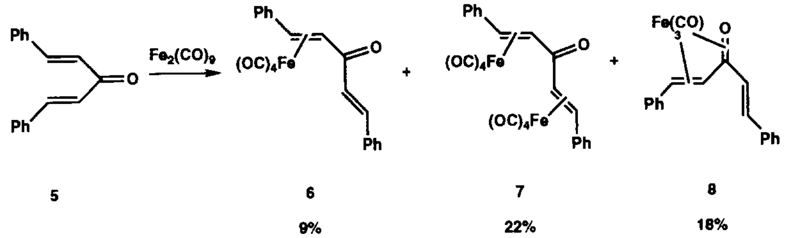

Scheme 2.

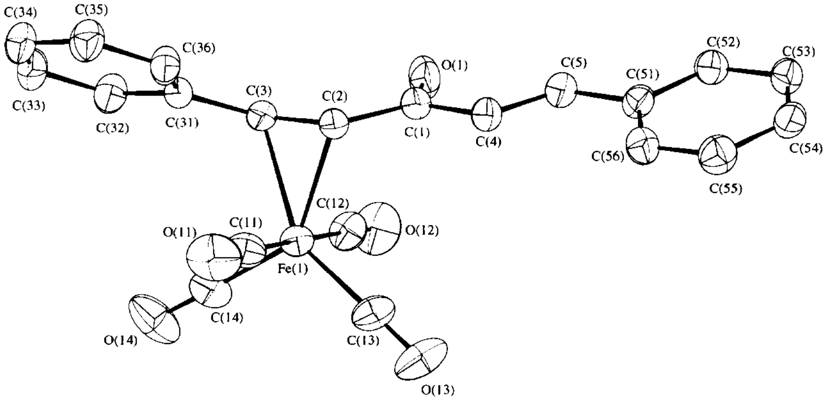

Fig. 1. The molecular structure and atom-numbers scheme for complex **6**.

Table 1
Bond lenghts (Å) and bond angles (deg) for $C_{21}H_{14}FeO_5$, (**6**)

Fe(1)–C(2)	2.105(2)	C(13)–O(13)	1.138(4)
Fe(1)–C(3)	2.138(2)	C(14)–O(14)	1.133(4)
Fe(1)–C(11)	1.808(3)	C(31)–C(32)	1.388(4)
Fe(1)–C(12)	1.827(3)	C(31)–C(36)	1.386(4)
Fe(1)–C(13)	1.803(3)	C(32)–C(33)	1.379(4)
Fe(1)–C(14)	1.794(3)	C(33)–C(34)	1.365(4)
C(1)–C(2)	1.472(3)	C(34)–C(35)	1.373(4)
C(1)–C(4)	1.484(4)	C(35)–C(36)	1.380(4)
C(1)–O(1)	1.227(3)	C(51)–C(52)	1.384(4)
C(2)–C(3)	1.409(3)	C(51)–C(56)	1.408(4)
C(3)–C(31)	1.482(3)	C(52)–C(53)	1.371(4)
C(4)–C(5)	1.313(4)	C(53)–C(54)	1.367(4)
C(5)–C(51)	1.464(3)	C(54)–C(55)	1.382(4)
C(11)–O(11)	1.129(3)	C(55)–C(56)	1.373(4)
C(12)–O(12)	1.120(3)		
C(2)–Fe(1)–C(3)	38.8(9)	C(2)–C(3)–C(31)	125.2(2)
C(2)–Fe(1)–C(11)	86.8(1)	C(1)–C(4)–C(5)	121.2(3)
C(3)–Fe(1)–C(11)	91.3(1)	C(4)–C(5)–C(51)	127.8(3)
C(2)–Fe(1)–C(12)	93.4(1)	Fe(1)–C(11)–O(11)	178.8(3)
C(3)–Fe(1)–C(12)	88.7(1)	Fe(1)–C(12)–O(12)	176.6(3)
C(11)–Fe(1)–C(12)	179.6(1)	Fe(1)–C(13)–O(13)	179.5(3)
C(2)–Fe(1)–C(13)	109.0(1)	Fe(1)–C(14)–O(14)	178.2(3)
C(3)–Fe(1)–C(13)	147.5(1)	C(3)–C(31)–C(32)	119.3(2)
C(11)–Fe(1)–C(13)	90.4(1)	C(3)–C(31)–C(36)	122.8(2)
C(12)–Fe(1)–C(13)	89.8(1)	C(32)–C(31)–C(36)	117.8(2)
C(2)–Fe(1)–C(14)	139.5(1)	C(31)–C(32)–C(33)	120.9(3)
C(3)–Fe(1)–C(14)	101.1(1)	C(32)–C(33)–C(34)	120.4(3)
C(11)–Fe(1)–C(14)	90.1(1)	C(33)–C(34)–C(35)	119.8(3)
C(12)–Fe(1)–C(14)	89.5(1)	C(34)–C(35)–C(36)	120.1(2)
C(13)–Fe(1)–C(14)	111.4(1)	C(31)–C(36)–C(35)	121.0(2)
C(2)–C(1)–C(4)	116.4(2)	C(5)–C(51)–C(52)	118.9(2)
C(2)–C(1)–O(1)	121.2(2)	C(5)–C(51)–C(56)	123.3(2)
C(4)–C(1)–O(1)	122.5(2)	C(52)–C(51)–C(56)	117.8(2)
Fe(1)–C(2)–C(1)	110.7(2)	C(51)–C(52)–C(53)	122.0(3)
Fe(1)–C(2)–C(3)	71.9(1)	C(52)–C(53)–C(54)	119.6(3)
C(1)–C(2)–C(3)	121.9(2)	C(53)–C(54)–C(55)	120.1(3)
Fe(1)–C(3)–C(2)	69.3(1)	C(54)–C(55)–C(56)	120.7(3)
Fe(1)–C(3)–C(31)	117.6(2)	C(51)–C(56)–C(55)	119.9(3)

E.S.D.s in parentheses refer to the last significant digit.

tems. The ^1H NMR spectrum exhibits signals, besides those for the aromatic protons, at δ 4.78 and 5.29 ppm (d, $J = 11.3$ Hz) as two doublets for the four vinylic protons. This upfield shift of the signals is also observed in the ^{13}C NMR spectrum: the carbons of the double bonds appear at δ 57.6 and 52.8 ppm, at almost the same frequency as complex **6**. The ORTEP view of complex **7** is depicted in Fig. 2, whereas the bond distances (Å) and the bond angles (deg) are listed in Table 2. The dinuclear complex **7** possesses a nearly perfect C_2 symmetry with the $Fe(CO)_4$ moieties and the phenyl rings lying on opposite faces of the fairly planar divinyl ketone. The geometry around each iron atom can be described as a slightly distorted trigonal bipyramid with the apical planes tilted by 69° and 47° with respect to the plane of the divinyl ketone. The C–C axis of the double bond lies in the equatorial plane: this geometry agrees well with that of mono-olefin $Fe(CO)_4$ and related dinuclear complexes, the structures of which have already been reported [9]. The C(2)–C(3) and C(4)–C(5) distances of the bound olefinic moieties, 1.390(9) and 1.394(7) Å are essentially the same, as are the distances of the vinylic carbons to the metal, whereas the bond angles around C(2), C(3), C(4), and C(5) show that there is an sp^2 hybridization.

Finally for complex **8** the ^1H NMR spectrum discloses signals, as for related η^4-vinyl ketone complexes [1,9,10], for the vinylic protons attached at C(2) and C(3) at respectively δ 3.44 and 6.28 ppm (d, $J = 9$ Hz), the signals for the protons attached to C(4) and C(5) giving a signal at δ 7.09 and 7.76 ppm (d, $J = 16$ Hz). The ^{13}C NMR spectrum shows signals for the carbons of the free double bond at δ 135.18 and 122.23 ppm and for the carbons of the coordinated double bond at δ 79.75 and 62.46 ppm. An X-ray study provided the molecular structure of complex **8**. Fig. 3 represents an ORTEP-like projection of the complex. Bond distances and angles are listed in Table 3. If the C(2)–C(3) and C(1)–O(1) bonds are both assumed to occupy a single-site coordination, the iron atom is five-fold coordinated with a distorted trigonal bipyramidal geometry. C(13) and O(1) atoms are in apical positions, with an angle around the metal centre of 165.4(3)°. This observed geometry is consistent with an η^4-coordination of the O(1)–C(1)–C(2)–C(3) moiety of the benzylideneacetone ligand to a $Fe(CO)_3$ fragment and is in good agreement with closely related compounds such as tetracarbonyl (cinnamaldehyde) iron(0) [11] and dicarbonyltriphenylphosphine (cinnamaldehyde) iron (0) [12]. As for complexes **6** and **7**, a lengthening of the coordinated double bond is observed, C(2)–C(3) = 1.411(13) Å compared with the free double bond: C(4)–C(5) = 1.331(12) Å. In contrast, the bond distance for the carbonyl group appears to be longer in complex **8** than in **6** and **7**, owing to the coordination to iron: C(1)–O(1) = 1.317(9) Å instead of 1.227(3) Å and 1.226(6) Å for **6** and **7** respectively.

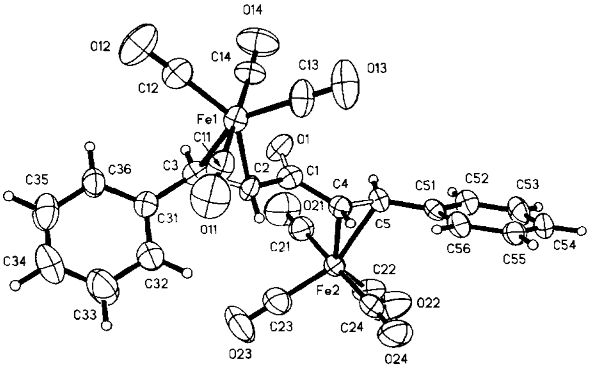

Fig. 2. The molecular structure and atom-numbers scheme for complex 7.

Table 2
Bond lenghts (A) and bond angles (deg) for $C_{25}H_{14}Fe_2O_9$, (**7**)

Fe(1)–C(11)	1.807(5)	O(1)–C(1)	1.226(6)
Fe(1)–C(12)	1.783(8)	C(1)–C(2)	1.491(7)
Fe(1)–C(13)	1.778(8)	C(1)–C(4)	1.472(9)
Fe(1)–C(14)	1.826(5)	C(2)–C(3)	1.390(9)
Fe(1)–C(2)	2.108(7)	C(3)–C(31)	1.486(7)
Fe(1)–C(3)	2.137(7)	C(4)–C(5)	1.394(7)
O(11)–C(11)	1.122(6)	C(5)–C(51)	1.479(9)
O(12)–C(12)	1.132(10)	C(31)–C(32)	1.374(8)
O(13)–C(13)	1.144(10)	C(31)–C(36)	1.379(9)
O(14)–C(14)	1.126(6)	C(32)–C(33)	1.372(10)
Fe(2)–C(21)	1.819(6)	C(33)–C(34)	1.345(12)
Fe(2)–C(22)	1.796(8)	C(34)–C(35)	1.361(10)
Fe(2)–C(23)	1.784(7)	C(35)–C(36)	1.377(9)
Fe(2)–C(24)	1.815(7)	C(51)–C(52)	1.380(7)
Fe(2)–C(4)	2.115(6)	C(51)–C(56)	1.387(7)
Fe(2)–C(5)	2.153(6)	C(52)–C(53)	1.373(10)
O(21)–C(21)	1.132(8)	C(53)–C(54)	1.381(8)
O(22)–C(22)	1.124(11)	C(54)–C(55)	1.358(9)
O(22)–C(23)	1.141(10)	C(55)–C(56)	1.384(9)
O(24)–C(24)	1.129(8)		

C(11)–Fe(1)–C(12)	90.0(3)	Fe(1)–C(13)–O(13)	177.6(5)
C(11)–Fe(1)–C(13)	89.4(3)	Fe(1)–C(14)–O(14)	173.6(7)
C(12)–Fe(1)–C(13)	111.5(3)	C(21)–Fe(2)–C(22)	88.3(3)
C(11)–Fe(1)–C(14)	178.1(3)	C(21)–Fe(2)–C(23)	91.8(3)
C(12)–Fe(1)–C(14)	88.7(3)	C(22)–Fe(2)–C(23)	111.2(4)
C(13)–Fe(1)–C(14)	89.8(3)	C(21)–Fe(2)–C(24)	176.9(3)
C(11)–Fe(1)–C(2)	89.4(3)	C(22)–Fe(2)–C(24)	88.6(3)
C(12)–Fe(1)–C(2)	139.2(3)	C(23)–Fe(2)–C(24)	89.7(3)
C(13)–Fe(1)–C(2)	109.3(3)	C(21)–Fe(2)–C(4)	94.4(3)
C(14)–Fe(1)–C(2)	92.6(3)	C(22)–Fe(2)–C(4)	140.4(3)
C(11)–Fe(1)–C(3)	91.4(3)	C(23)–Fe(2)–C(4)	108.2(3)
C(12)–Fe(1)–C(3)	101.0(3)	C(24)–Fe(2)–C(4)	87.7(3)
C(13)–Fe(1)–C(3)	147.5(3)	C(21)–Fe(2)–C(5)	87.7(3)
C(14)–Fe(1)–C(3)	90.2(3)	C(22)–Fe(2)–C(5)	102.8(3)
C(2)–Fe(1)–C(3)	38.2(2)	C(23)–Fe(2)–C(5)	146.0(3)
Fe(1)–C(11)–O(11)	178.4(7)	C(24)–Fe(2)–C(5)	92.6(3)
Fe(1)–C(12)–O(11)	178.3(6)	C(4)–Fe(2)–C(5)	38.1(2)
Fe(2)–C(21)–O(21)	175.3(7)	C(4)–C(5)–C(51)	125.7(4)
Fe(2)–C(22)–O(22)	179.8(7)	C(3)–C(31)–C(32)	122.6(6)
Fe(2)–C(23)–O(23)	178.8(6)	C(3)–C(31)–C(36)	120.4(5)
Fe(2)–C(24)–O(24)	178.5(6)	C(32)–C(31)–C(36)	117.0(6)
0(1)–C(1)–C(2)	121.2(6)	C(31)–C(32)–C(33)	121.5(7)
0(1)–C(1)–C(4)	123.2(5)	C(32)–C(33)–C(34)	120.9(7)
C(2)–C(1)–C(4)	115.6(4)	C(33)–C(34)–C(35)	119.0(7)
Fe(1)–C(2)–C(1)	113.2(4)	C(34)–C(35)–C(36)	120.7(7)
Fe(1)–C(2)–C(3)	72.0(4)	C(31)–C(36)–C(35)	120.9(6)
C(1)–C(2)–C(3)	122.7(4)	C(5)–C(51)–C(52)	119.9(4)
Fe(1)–C(3)–C(2)	69.8(4)	C(5)–C(51)–C(56)	122.3(5)
Fe(1)–C(3)–C(31)	115.9(4)	C(52)–C(51)–C(56)	117.7(6)
C(2)–C(3)–C(31)	125.0(5)	C(51)–C(52)–C(53)	121.1(5)
Fe(2)–C(4)–C(1)	108.1(4)	C(52)–C(53)–C(54)	19.5(7)
C(1)–C(4)–C(5)	123.4(4)	C(54)–C(55)–C(56)	120.3(5)
Fe(2)–C(5)–C(4)	69.5(3)	C(51)–C(56)–C(55)	121.0(5)
Fe(2)–C(5)–C(51)	114.7(4)		

E.S.D.s in parentheses refers to the last significant digit.

Easy interconversion between the various complexes is observed: thus an acetone solution of complex **7** leads to complex **8** (7%) after 24 h at room temperature, and refluxing **7** in THF for 1.5 h gives a 16% yield of complex **6** and complex **8** as a by product. Moreover, refluxing complex **6** in THF for 2 h leads to complex **8** in a 17% yield (Scheme 3).

2.2. Reaction of complexes 6, 7, and 8 with MeLi / CO: formation of the ketene complex 9 and of the μ-alkylidene complex 10

The purpose of this investigation was to prepare the new ketene complex $Fe(CO)_4(\eta^4\text{-}PhCH{=}CH(C{=}C{=}O)CH{=}CHPh)$ (**9**) and to try to bring to light a possible influence of the supplementary double bond of the starting complexes **6**, **7**, and **8** on the course of the reaction.

Thus, treatment of the dinuclear complex **7** with methyl lithium under an atmosphere of CO, as reported in the literature [1], led to two new complexes which were easily detected by thin layer chromatography (TLC). Silica-gel chromatography of the reaction mixture gave a product, isolated as an orange solid in 25% yield, which proved to be the η^4-vinyl ketene complex **9**, in agreement with its spectroscopic data. The mass spectrum confirmed the presence of one metal centre and the substitution of the ketone oxygen atom by one CO group. Whereas the ^1H NMR spectrum disclosed signals for the hydrogens of a free double bond at δ 7.14 ppm (d, $J = 16$ Hz), 6.47 ppm (d, $J = 16$ Hz) and a coordinated double bond at δ 6.52 ppm (d, $J = 9.5$ Hz) and 3.48 ppm (d, $J = 9.5$ Hz), in the ^{13}C NMR spectrum, one observes the characteristic signals for a coordinated vinyl ketene, at δ 233.7 (C=O), 92.9 (C=C=O), and for the coordinated double bond at δ 48.9 and 60.5 ppm [1].

For the less polar product, a red complex $Fe_2(CO)_6(\mu\text{-}\eta^3, \eta^3\text{-}C(CH{=}CHPh)_2)$ (**10**) obtained in a 9% yield, both the elemental analysis and the mass spectrum agreed with the presence of two metal centres. Indeed, the mass spectrum displayed ions owing to the successive loss of six CO groups (M^+ to $M^+ - 6CO$).

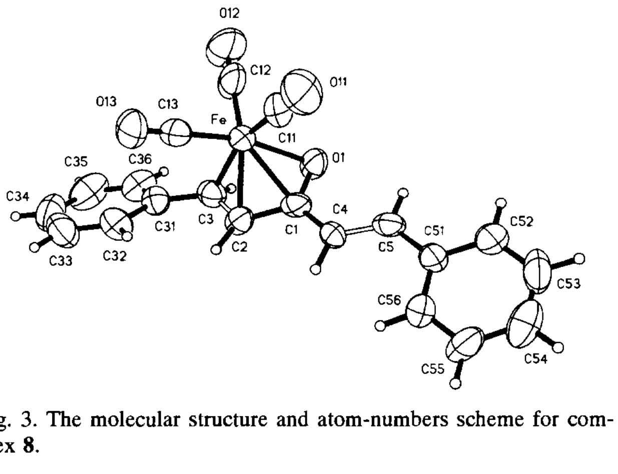

Fig. 3. The molecular structure and atom-numbers scheme for complex **8**.

Moreover, no ketone νCO appeared in the IR. The ^{1}H NMR spectrum disclosed signals, besides those for two phenyl groups, at δ 6.48 and 3.61 ppm as two doublets (d, $J = 9$ Hz), owing to two coordinated double bonds. This means that the newly formed complex must be highly symmetrical. The presence of these two coordinated double bonds was also confirmed by the ^{13}C NMR spectrum which showed two signals at δ 72.4 and 67.6 ppm. An additional signal owing to a quaternary carbon atom appeared at δ 112.3 ppm, suggesting that deoxygenation of the carbonyl group occurred. The structure of this complex was finally assessed by an X-ray diffraction study. Its ORTEP projection appears in Fig. 4, whereas the bond distances (Å) and the bond angles (deg) are gathered in Table 4.

The most important feature of complex **10** is that the organic ligand is the result of the deoxygenation of the starting dibenzylideneacetone, giving rise to a distyrylcarbene moiety which bridges the two metal centres. The complex displays a perfect C_2 symmetry, a fact which explains the very simple ^{1}H and ^{13}C NMR spectra. It can be described either as a μ-alkylidene complex bearing two coordinated double bonds or as a bis-π-allyl system, one carbon atom being common to

Table 3
Bond lenghts (A) and bond angles (deg) for $C_{20}H_{14}FeO_4$ (**8**)

Fe–C(11)	1.815(11)	C(4)–C(5)	1.331(12)
Fe–C(12)	1.813(10)	C(5)–C(51)	1.467(13)
Fe–C(13)	1.776(8)	C(31)–C(32)	1.394(12)
Fe–O(1)	2.020(5)	C(31)–C(36)	1.370(13)
Fe–C(1)	2.093(8)	C(32)–C(33)	1.388(13)
Fe–C(2)	2.082(8)	C(33)–C(34)	1.377(15)
Fe–C(3)	2.141(9)	C(34)–C(35)	1.362(18)
O(11)–C(11)	1.126(13)	C(35)–C(36)	1.372(15)
O(12)–C(12)	1.136(12)	C(51)–C(52)	1.390(13)
O(13)–C(13)	1.136(10)	C(51)–C(56)	1.384(13)
O(1)–C(1)	1.317(9)	C(52)–C(53)	1.377(15)
C(1)–C(2)	1.420(12)	C(53)–C(54)	1.339(17)
C(1)–C(4)	1.449(12)	C(54)–C(55)	1.365(15)
C(2)–C(3)	1.411(13)	C(55)–C(56)	1.371(13)
C(3)–C(31)	1.469(13)		
C(11)–Fe–C(12)	105.1(4)	Fe–C(13)–O(13)	178.1(7)
C(11)–Fe–C(13)	87.8(4)	Fe–O(1)–C(1)	74.4(4)
C(12)–Fe–C(13)	96.3(4)	Fe–C(1)–O(1)	68.3(4)
C(11)–Fe–O(1)	93.8(4)	Fe–C(1)–C(2)	69.7(5)
C(12)–Fe–O(1)	97.3(3)	O(1)–C(1)–C(2)	115.5(8)
C(13)–Fe–O(1)	165.4(3)	Fe–C(1)–C(4)	133.1(6)
C(11)–Fe–C(1)	93.0(4)	O(1)–C(1)–C(4)	122.8(7)
C(12)–Fe–C(1)	132.8(4)	C(2)–C(1)–C(4)	121.6(7)
C(13)–Fe–C(1)	128.1(3)	Fe–C(2)–C(1)	70.5(5)
O(1)–Fe–C(1)	37.3(3)	Fe–C(2)–C(3)	72.8(5)
C(11)–Fe–C(2)	120.9(4)	C(1)–C(2)–C(3)	118.0(8)
C(12)–Fe–C(2)	132.1(4)	Fe–C(3)–C(2)	68.2(5)
C(13)–Fe–C(2)	98.0(3)	Fe–C(3)–C(31)	125.1(6)
O(1)–Fe–C(2)	68.7(3)	C(2)–C(3)–C(31)	126.0(8)
C(1)–Fe–C(2)	39.8(3)	C(1)–C(4)–C(5)	122.9(7)
C(11)–Fe–C(3)	159.9(4)	C(4)–C(5)–C(51)	126.3(7)
C(12)–Fe–C(3)	94.5(4)	C(3)–C(31)–C(32)	120.6(8)
C(13)–Fe–C(3)	94.5(3)	C(3)–C(31)–C(36)	121.8(8)
O(1)–Fe–C(3)	79.1(3)	C(32)–C(31)–C(36)	117.6(8)
C(1)–Fe–C(3).	69.9(4)	C(31)–C(32)–C(33)	120.5(8)
C(2)–Fe–C(3)	39.0(3)	C(32)–C(33)–C(34)	119.6(10)
Fe–C(11)–O(11)	177.6(9)	C(33)–C(34)–C(35)	120.5(10)
Fe–C(12)–O(12)	177.1(8)	C(34)–C(35)–C(36)	119.3(10)
C(31)–C(36)–C(35)	122.5(9)	C(52)–C(53)–C(54)	120.7(10)
C(5)–C(51)–C(52)	120.8(8)	C(53)–C(54)–C(55)	120.0(10)
C(5)–C(51)–C(56)	122.7(8)	C(54)–C(55)–C(56)	120.0(10)
C(52)–C(51)–C(56)	116.5(8)	C(51)–C(56)–C(55)	121.7(9)
C(51)–C(52)–C(53)	121.1(9)		

E.S.D.s in parentheses refers to the last significant digit.

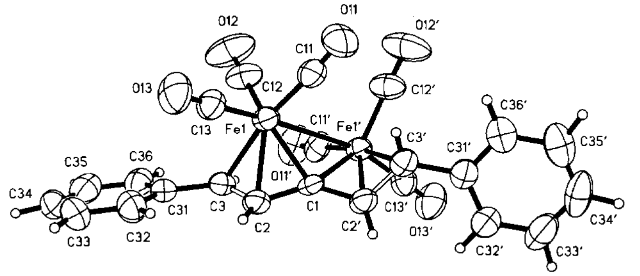

Fig. 4. The molecular structure and atom-numbers scheme for complex **10**.

the two allylic groups (Scheme 4). The angle between the Fe(1)–C(1)–Fe(1′) and C(2)–C(1)–C(2′) planes is 39.6° while that between the C(1)–C(2)–C(3) and C(1)–C(2′)–C(3′) planes is 52.3°. The internuclear distance, Fe–Fe = 2.781(1) Å is within the limits for weak single bonds [13]. To our knowledge, it is the largest Fe–Fe distance observed for this type of complex [14,15]. This fact is also reflected in the large Fe(1)–C(1)–Fe(1′) angle observed for complex **10**, very close to 90° (88.9(2)°), comparable with the angle of 83(1)° observed in the structure of octacarbonyldiphenyl (vinylidene) di-iron(0) [15].

Complex **13** had already been obtained, with similar structural features, in this laboratory starting from the μ-methylene complex **12**, upon insertion of two molecules of acetylene (Scheme 5) [16]. Interestingly, the bond distances around the metal centres for the two complexes **13** and **10** are similar. Thus the internuclear distance is 2.776(1) Å in complex **13** and 2.781(1) in complex **10**, the distances of the bridging carbon to the metals are 1.992(5) Å for **13** and 1.985(4) Å for **10**. A significant difference is, however, observed for the distances of the terminal carbons of the allylic groups from the metals which are slightly longer, 2.210(5) Å in **10** rather than 2.089(4) Å in **13**.

Table 4
Bond lenghts (A) and bond angles (deg) for $C_{23}H_{14}Fe_2O_6$, (**10**)

Fe(1)–C(11)	1.783(6)	C(1)–C(2)	1.389(5)
Fe(1)–C(12)	1.792(5)	C(2)–C(3)	1.392(6)
Fe(1)–C(13)	1.774(4)	C(3)–C(31)	1.474(6)
Fe(1)–C(1)	1.985(4)	C(31)–C(32)	1.394(6)
Fe(1)–C(2)	2.089(4)	C(31)–C(36)	1.377(7)
Fe(1)–C(3)	2.210(5)	C(32)–C(33)	1.370(8)
Fe(1)Fe(1′)	2.781(1)	C(33)–C(34)	1.354(9)
0(11)–C(11)	1.150(7)	C(34)–C(35)	1.357(9)
O(12)–C(12)	1.146(6)	C(35)–C(36)	1.385(7)
O(13)–C(13)	1.145(6)		
C(11)–Fe(1)–C(12)	99.5(2)	Fe(1)–C(11)–O(11)	175.9(4)
C(11)–Fe(1)–C(13)	89.9(2)	Fe(1)–C(12)–O(12)	178.8(5)
C(12)–Fe(1)–C(13)	97.5(2)	Fe(1)–C(13)–O(13)	177.1(4)
C(11)–Fe(1)–C(1)	99.7(2)	Fe(1)–C(1)–C(2)	74.2(2)
C(12)–Fe(1)–C(1)	134.3(2)	Fe(1)–C(1)–Fe(1′)	88.9(2)
C(13)–Fe(1)–C(1)	123.4(2)	C(2)–C(1)–Fe(1′)	138.2(3)
C(11)–Fe(1)–C(2)	132.1(2)	C(2)–C(1)–C(2′)	141.4(5)
C(12)–Fe(1)–C(2)	126.5(2)	Fe(1)–C(2)–C(1)	66.1(2)
C(13)–Fe(1)–C(2)	95.7(2)	Fe(1)–C(2)–C(3)	75.9(2)
C(1)–Fe(1)–C(2)	39.8(2)	C(1)–C(2)–C(3)	120.1(4)
C(11)–Fe(1)–C(3)	169.4(2)	Fe(1)–C(3)–C(2)	66.5(3)
C(12)–Fe(1)–C(3)	89.8(2)	Fe(1)–C(3)–C(31)	124.4(3)
C(13)–Fe(1)–C(3)	93.9(2)	C(2)–C(3)–C(31)	125.1(4)
C(1)–Fe(1)–C(3)	69.9(1)	C(3)–C(31)–C(32)	122.6(4)
C(2)–Fe(1)–C(3)	37.6(2)	C(3)–C(31)–C(36)	119.3(4)
C(11)Fe(1)Fe(1′)	82.9(1)	C(32)–C(31)–C(36)	118.1(4)
C(12)–Fe(1)–Fe(1′)	97.0(2)	C(31)–C(32)–C(33)	120.2(5)
C(13)Fe(1)Fe(1′)	164.7(1)	C(32)–C(33)–C(34)	121.3(5)
C(1)–Fe(1)–Fe(1′)	45.5(1)	C(33)–C(34)–C(35)	119.4(6)
C(2)–Fe(1)–Fe(1′)	79.5(1)	C(34)–C(35)–C(36)	120.8(5)
C(3)–Fe(1)–Fe(1′)	91.0(1)	C(31)–C(36)–C(35)	120.3(5)

Primed atoms generated by. 1-*x*, *y*, 1.5-*z*.
E.S.D.s in parentheses refers to the last significant digit.

Similar results were observed starting either from complex **8** which gave complexes **9** and **10** in, respec-

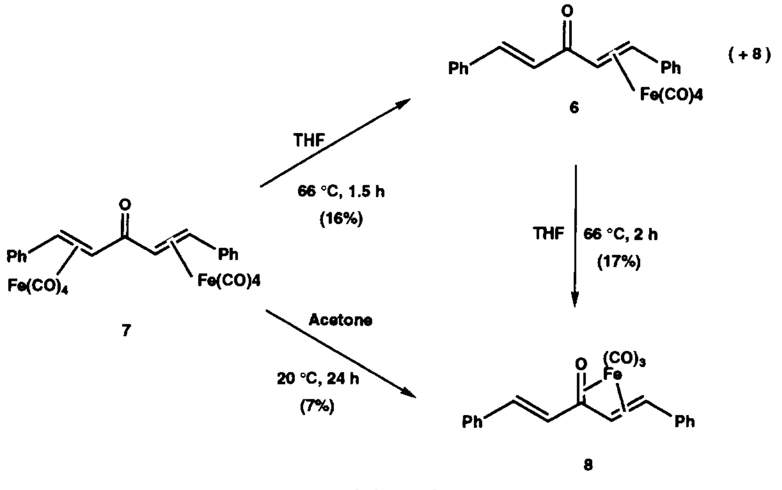

Scheme 3.

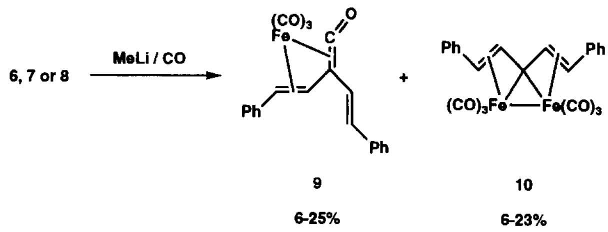

Scheme 4.

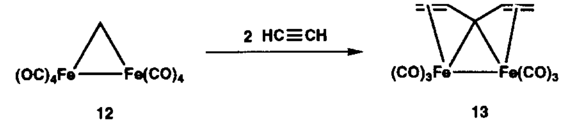

Scheme 5.

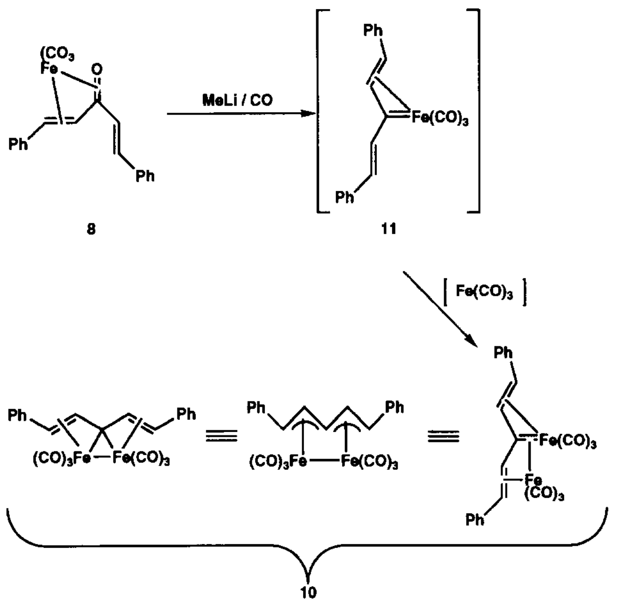

Scheme 6.

tively, 18% and 6.5% yields, or from complex **6** which gave the same complexes as **7** in a 23% yield.

3. Conclusion

Although the formation of a stable $Fe_2(CO)_8(\mu\text{-}\eta^2,\eta^2$-dibenzylideneacetone) complex is remarkable, the most interesting result is the transformation of this complex and also of complexes **6** and **8** into a distyrylcarbene complex **10**. Indeed this complex can be considered as the result of the stabilization of the suspected mononuclear alkylidene complex **11** by $Fe(CO)_3$ (Scheme 6). The key for the success of this reaction is probably the presence of an extra double bond in the starting vinyl ketone complex and thus in the intermediate **11**. Previous observations [17] from this laboratory have indeed indicated that conjugated mononuclear carbene complexes of iron, and of tungsten, similar to complex **11** could be coordinated to a $Fe(CO)_3$ fragment to produce either homodinuclear or heterodinuclear μ-alkylidene complexes: such a reaction probably occurs in the transformations described herein. Intermediates related to complex **10** have been proposed in other reactions, generally without direct evidence for the formation of these transient species [3,18].

Finally, it was possible for the first time to prepare an η^4-vinyl ketene complex **9**, starting from η^2-mono or di-nuclear reagents (complexes **6** or **7**), probably via the η^4-vinyl ketone complex **8**.

4. Experimental

4.1. General methods

^1H NMR and ^{13}C NMR spectra were recorded on a Varian VXR-300S spectrometer, JEOL GX 400 or BRUKER WM 200. IR spectra were recorded on a Perkin–Elmer 283B or 1420 spectrometer and mass spectra on a ZAB HSQ (Fisons) instrument. Microanalyses were performed by the Service Central d'Analyses du CNRS, Solaize. Melting points were measured using a Mel-Temp II apparatus and are uncorrected. Column chromatography was performed with Merck silica gel (70–230 mesh) using various ratios of ethyl acetate/hexane or dichloromethane/hexane as eluent. All reagents were obtained from commercial suppliers and used as received. Reactions were performed under a nitrogen atmosphere in carefully dried glassware. Benzene, tetrahydrofuran (THF) and diethyl ether were distilled from sodium/benzophenone ketyl under an argon atmosphere.

4.2. Obtaining complexes 6, 7 and 8

Complexes $Fe(CO)_4[\eta^2(CO)(CH{=}CHPh)_2]$ (**6**), $Fe_2(CO)_8$ $[\eta^2, \eta^2(CO)(CH{=}CHPh)_2]$ (**7**) and $Fe(CO)_4[\eta^4(CO)(CH{=}CHPh)_2]$ (**8**) were obtained from dibenzylideneacetone (**5**) (8 g, 34.2 mmol) in anhydrous diethyl ether to which $Fe_2(CO)_9$ (13.68 g, 37.6 mmol) was added. After stirring at room temperature for 24 h, under nitrogen, a yellow solid precipitated. Filtration of the suspension gave yellow crystals of complex **7** (4.24 g, 22% resp. dibenzylideneacetone) and a solution from which the solvent was evaporated under vacuum. Silica-gel chromatography of the residue with ethyl acetate/hexane (5/95) as the eluent first gave complex **8** (2.27 g, 18%) as an orange solid, then complex **7** (1.12 g, 6%) and finally complex **6** (1.27 g, 9%) as a yellow solid.

Complex **6**: mp, 104 °C; IR ($CHCl_3$), 2095 cm^{-1}, 2015 cm^{-1}, 1985 cm^{-1} (M − CO), 1665 cm^{-1} (CO);

^{1}H NMR (200 MHz, $CDCl_3$) δ 4.59 (1H, d, $J = 11.3$ Hz), 5.33 (1H, d, $J = 11.3$ Hz), 7.04–7.81 (m, 12H, Ar, C=C); ^{13}C NMR (50 MHz, $CDCl_3$) δ 207.1 (CO), 193.6 (CO), 141.9, 134.8, 130.3, 128.9, 128.8, 128.3, 126.7, 126.1, 125.7 (Ar, C=C), 57.7, 53.3 [Fe(C=C)]. HRMS for $C_{18}H_{14}FeO_2$: ($M^+ - 3CO$) calc., 318.0343; found, 318.0341. Anal. Found: C, 62.02; H, 3.64; Calc. for $C_{21}H_{14}FeO_5$: C, 62.69; H, 3.48.

Complex **7**: mp, 130 °C; IR (KBr), 2098 cm^{-1}, 2022 cm^{-1}, 2002 cm^{-1}, 1982 cm^{-1}, 1972 cm^{-1} (M – CO), 1630 cm^{-1} (CO). ^{1}H NMR (200 MHz, $CDCl_3$) δ 7.39–7.17 (m, 10H, Ar), 5.3 (d, 2H, $J = 11.2$ Hz, =CHCO), 4.78 (d, 2H, $J = 11.2$ Hz, PhCH=C); ^{13}C NMR (50 MHz, $CDCl_3$) δ 207.3 (M – CO), 184.0 (CO), 141.8, 128.9, 128.3, 126.7, 126.2 (Ar), 57.6, 52.8 (FeCH=CH). Anal. Found: C, 51.76; H, 2.62. Calc. for $C_{25}H_{14}Fe_2O_9$: C, 52.63; H, 2.46. MS (FAB): 571 (MH^+), 542 ($M^+ - CO$), 514 ($M^+ - 2CO$), 346 ($M^+ - 8CO$).

Complex **8**: mp, 100 °C; IR (KBr), 2065 cm^{-1}, 2002 cm^{-1}, 1990 cm^{-1}, 1985 cm^{-1} (M – CO), 1630 cm^{-1} (CO); ^{1}H NMR (200 MHz, $CDCl_3$) δ 7.80–7.05 (m, 12H, Ar, CH=CH), 6.28 (d, 1H, $J = 9$ Hz), 3.44 (d, 1H, $J = 9$ Hz); ^{13}C NMR (50 MHz, $CDCl_3$) δ 207.2 (M – CO), 143.4, 138.5, 135.1–122.2 (Ar, C=C), 79.7, 62.5 (FeCH=CH). HRMS for $C_{20}H_{14}FeO_4$: (M^+), 374.0241; found, 374.0239.

Complex **7** was also obtained from dibenzylideneacetone (4 g, 17.1 mmol) in diethyl ether (150 ml) and $Fe_2(CO)_9$ (6.84 g, 18.8 mmol) at reflux temperature for 24 h. Filtration of the solution over alumina gave complex **7** (2.35 g, 24%) as a yellow solid. Silica-gel chromatography of the residue obtained after evaporation of the solvent under vacuum with hexane/ethyl acetate (70/30) produced a further fraction of complex **7** (0.88 g). Total yield of **7**, 33%.

4.3. Formation of complex 8 from complex 7

Complex **7** (1.140 g, 2 mmol) was kept at room temperature in acetone (150 ml) for 24 h. After filtration of the solution over neutral alumina, the solution was evaporated under vacuum and the residue chromatographed on silica gel with hexane/ethyl acetate (99/1) as eluent. Evaporation of the appropriate fractions gave complex **8** (0.050 g, 7%).

4.4. Formation of complex 6 from complex 7

A solution of complex **7** (0.67 g, 1.18 mmol) in THF (100 ml) was refluxed for 1.5 h. The solution was evaporated under vacuum and the residue chromatographed on silica gel to give complex **6** (0.070 g, 16%), identical with an authentic sample in all respects. A by-product could be detected by TLC and was identified as complex **8**.

4.5. Formation of complex 8 from complex 6

Compound **6** (0.402 g, 1 mmol) was dissolved in THF (50 ml) and was refluxed for 2 h. Filtration over alumina yielded an orange solution containing pure complex **8** (TLC), which after reduction afforded 65 mg of **8** (17%).

4.6. Formation of complex $Fe(CO)_4(\eta^4\text{-}PhCH=CH(C=C=O)CH=CHPh)$ (9) and complex $Fe_2(CO)_6[\mu\text{-}\eta^3, \eta^3\text{-}C(CH=CHPh)_2]$ (10)

From complex 7. A solution of complex **7** (5.7 g, 10 mmol) in THF (100 ml) was cooled to – 78 °C and kept under a slight overpressure of CO (ca. 1.1 atm). Methyl lithium (5.4 ml, 1.4 M in Et_2O) was then added. The solution was kept at this temperature for 1 h, then allowed to heat to room temperature for 3 h. Evaporation of the solvent under vacuum, followed by silica-gel chromatography of the residue with hexane/ethyl acetate (98/2) as eluent, first gave complex **10** (0.435 g, 9%) as a red solid: mp, 200 °C; IR (KBr), 2040 cm^{-1}, 1998 cm^{-1}, 1965 cm^{-1}, 1950 cm^{-1}; ^{1}H NMR (200 MHz, $CDCl_3$) δ 7.42–7.32 (m, 10H, Ar), 6.48 (d, 2H, $J = 9$ Hz), 3.61 (d, 2H, $J = 9$ Hz); ^{13}C NMR (50 MHz, $CDCl_3$) δ 210.6 (CO), 138.8, 128.0, 127.7, 127.2 (Ar), 112.3 (CFe_2), 72.4, 67.6 (C=C). Anal. Found: C, 55.25; H, 3.01. Calc. for $C_{23}H_{14}Fe_2O_6$: C, 55.42; H, 2.81. HRMS for $C_{23}H_{14}Fe_2O_6$: (M^+), 497.9489; found, 497.9491.

Elution with the same solvent gave complex **9** (0.96 g, 25%) as orange crystals: mp, 143 °C (dec); IR (KBr), 2062 cm^{-1}, 2002 cm^{-1} (M – CO), 1766 cm^{-1} (CO); ^{1}H NMR (200 MHz, $CDCl_3$), δ 7.47–7.25 (m, 10H, Ar), 7.14 (d, 1H, $J = 16$ Hz, C(O)C*H*=CHPh), 6.47 (d, 1H, $J = 16$ Hz, C(O)CH=C*H*Ph), 6.52 (d, 1H, $J = 9.5$ Hz, Fe(CH=C*H*C(O)), 3.48 (d, 1H, $J = 9.5$ Hz, Fe(C*H*=CHCO)); ^{13}C NMR (50 MHz, $CDCl_3$) δ 233.7 (C=*C*=O), 208.0 (CO), 137.9, 135.7, 129.2, 128.8, 128.7, 127.7, 126.6 (Ar), 135.9 (*C*=C–CCO), 118.3 (*C*=C=O), 92.9 (Fe*C*H=C), 60.5(Fe*C*Ph=C), 48.9 (*C*=C=O). HRMS for $C_{20}H_{14}FeO_3$: ($M^+ - CO$), 358.0292; found, 358.0292.

From complex 8. A solution of complex *8* (2 g, 5.3 mmol) in THF (100 ml) was treated as above with MeLi (3.8 ml, 1.4 M in Et_2O). Silica-gel chromatography gave complexes **9** (0.370 g, 18%) and **10** (0.17 g, 6.5%).

From complex 6. A solution of complex **6** (1 g, 2.48 mmol) in THF (50 ml) was treated as above with MeLi (1.7 ml, 1.4 M in Et_2O). A work up as above gave complexes **10** (0.084 g, 7%), and **9** (0.22 g, 23%).

4.7. X-ray data collection, structure solution and refinements

Suitable crystals of complexes **6**, **7**, **8** and **10** were grown by slow cooling hexane/dichloromethane solu-

Table 5
Crystal data and refinement details for complexes **6**, **7**, **8** and **10**

Compound	**6**	**7**	**8**	**10**
Formula	$C_{21}H_{14}FeO_5$	$C_{25}H_{14}Fe_2O_9$	$C_{20}H_{14}FeO_4$	$C_{23}H_{14}Fe_2O_6$
M_w	402.2	570.1	374.2	498.0
Crystal system	Monoclinic	Triclinic	Orthorhombic	Orthorhombic
Space group	$P2_1/n$	$\bar{P}1$	Pbca	Pbcn
a (Å)	6.326(2)	9.677(5)	13.397(2)	17.155(4)
b (Å)	14.567(2)	10.635(5)	10.041(3)	7.842(2)
c (Å)	20.504(2)	13.471(6)	26.579(2)	15.857(2)
α (deg)	104.24(3)			
β (deg)	96.91(2)	105.46(4)		
γ (deg)	104.75(4)			
U (Å^3)	1875(4)	1216.7(8)	3575.1(8)	2133.2(5)
Z	4	2	8	4
D_c (g cm^3)	1.42	1.56	1.39	1.55
μ (cm^{-1})	8.28	100.6	8.63	14.0
F (000)	825.4	576	1536	1008
Diffractometer	Enraf CAD4F	Nicolet P3	Siemens P3/PC	Siemens P3/PC
Radiation	Mo Kα	Cu Kα	Mo Kα	Mo Kα
Scan type	ω-2θ	θ/2θ	ω-2θ	ω-2θ
Scan range (deg)	$1.5 < 2\theta < 25$	$3 < 2\theta < 100$	$3 < 2\theta < 50$	$3 < 2\theta < 60$
Data collected	3789	2704	3146	2819
Data used (Criterion)	2481($F > 3\sigma(F)$)	2508 ($F > 3\sigma(F)$)	1284 ($F > 4\sigma(F)$)	1392 ($F > 3\sigma(F)$)
$R(R_w)$ (%)	3.28 (3.89)	5.1 (5.7)	5.42 (5.68)	4.46 (5.16)
l.s. parameters	289	167	239	148
G.O.F.	1.12	1.06	1.13	1.08

tions to 0 °C. A crystal summary is given in Table 5. As a general procedure, for each compound the accurate cell dimensions and orientation matrix were obtained from least-squares refinement of the setting angles of 25 well-defined reflections. Diffraction intensities were collected at room temperature and all data were corrected for the usual Lorentz and polarization effects and placed on an approximately absolute scale. Absorption correction was applied by DIFABS [19] for complexes **6** (min./max. correction, 0.61–1) and **7** (min./max. correction, 0.69–1.19). An empirical absorption correction [20] was applied for complexes **8** and **10** (correction factors in the range 0.68–0.78 and 0.56–0.81 respectively). The space groups for **6**, **8** and **10** were determined from systematic absences. The structures were solved by direct methods followed by different Fourier maps, and refined by full-matrix least-squares. All non-hydrogen atoms were refined anisotropically to convergence. Hydrogen atoms were located on difference Fourier syntheses for complex **6**. Their atomic coordinates were refined and they were assigned an overall isotropic thermal parameter. Hydrogen atoms were included as an idealized isotropic contribution (riding model) for complexes **7**, **8** and **10**. Data reduction and structure solution were achieved using CRYSTALS [21] for complex **6** and the SHELXTL PLUS structure solution software package [22] for others. Analytical scattering factors for neutral atoms were taken from Ref. [23].

Tables showing fractional coordinates (Tables S1–S4), anisotropic thermal parameters (Tables S5–S8), hydrogen-atom parameters (Tables S9–S12) and structure factors (Tables S13–S16) for complexes **6**, **7**, **8** and **10** are available from the authors (49 pp.).

Acknowledgments

Acknowledgments are made to CONACyT (Mexico), to the European Communities (ISC Programme) and to CNRS (France) for financial support. Acknowledgments are due to Marisol Cervantes Vázquez and Aída Díaz Aquino for the synthesis of complex **9**.

References

[1] N.W. Alcock, C.J. Richards and S.E. Thomas, *Organometallics, 10* (1991) 231, and references cited therein.

[2] C. Alvarez, A.C.Cano, R.A. Toscano, A. Parlier and H. Rudler, *Bull. Soc. Chim. Fr., 130* (1993) 601.

[3] T.A. Mitsudo, H. Watanabe, T. Sasaki, Y. Takegami, Y. Watanabe, K. Kafuku and K. Nakatsu, *Organometallics, 8* (1989) 368, and references cited therein.

[4] J. Klimes and E. Weiss, *Angew. Chem. Int. Ed. Engl., 21* (1982) 205.

[5] E. Chelain, R. Goumont, L. Hamon, A. Parlier, M. Rudler, H. Rudler, J.-C. Daran and J. Vaissermann, *J. Am. Chem. Soc., 114* (1992) 8088.

[6] E. Chelain, A. Parlier, M. Audouin, H. Rudler, J.-C. Daran and J. Vaissermann, *J. Am. Chem. Soc., 115* (1993) 10568.

[7] The structure of complex 7 was reported as a preliminary

communication: A.C. Cano, N. Zuñiga-Villareal, C. Alvarez, R.A. Toscano, M. Cervantes, A. Díaz and H. Rudler, *J. Organomet. Chem.*, *464* (1994) C23.

[8] (a) E. Weiss, K. Stark, J.E. Lancaster and H.D. Murdoch., *Helv. Chim. Acta*, *46* (1963), 288; (b) K. Stark, J.E. Lancaster, H.D. Murdoch and E. Weiss, *Z. Naturforsch*, *B19* (1964) 284.

[9] (a) J.A.S. Howell, B.F.G. Johnson, P.L. Josty and J.Lewis, *J. Organomet. Chem.*, *39* (1972) 329; (b) E. Koerner von Gustorf, F.-W. Grevels, C. Krüger and G. Olbrich, *Z. Naturforsch*, *B27* (1972) 392; (c) A.M. Brodie, B.F.G. Johnson, P.L. Josty and J. Lewis, *J. Chem. Soc., Dalton Trans,* (1972) 2031.

[10] (a) E. Koerner von Gustorf, O. Jaenicke and O.E. Polansky, *Z. Naturforsch*, *B27* (1972) 575; (b) A.N. Nesmeyanov, L.V. Rybin, N.T. Gubenko, M.I. Rybinskaya and P.V. Petrovskii, *J. Organomet. Chem.*, *71* (1974) 271; (c) M.S. Brookhart, G.W. Koszalka, G.O. Nelson, G. Scholes and R.A. Watson, *J. Am. Chem. Soc*, *98* (1976) 8155; (d) K.K. Joshi, *J. Chem. Soc. (A)*, (1966) 594; (e) H. Alper and J.T. Edward, *J. Organomet. Chem.*, *16* (1969) 342.

[11] A. de Cian and R. Weiss, *Acta Crystallogr.*, *B28* (1972) 3273.

[12] M. Sacerdoti, V. Bertolasi and G. Gilli, *Acta Crystallogr. B36* (1980) 1061.

[13] *Comprehensive Organometallic Chemistry*, in Sir G. Wilkinson (ed.), Pergamon, Oxford, 1982, Vol. 4, p. 513.

[14] (a) G. Dettlaf, U. Behrens and E. Weiss, *Chem. Ber.*, *111* (1978) 3019; (b) R. Aumann, G. Henkel and B. Krebs, *Angew. Chem., Int. Ed. Engl.*, *21* (1982) 204.

[15] O.S. Mills and A.D. Redhouse, *J. Chem. Soc. (A)*, (1968) 1282.

[16] D. Navarre, A. Parlier, H. Rudler and J.C. Daran, *J. Organomet. Chem.*, *322* (1987) 103.

[17] C. Alvarez, A. Parlier, F. Rose-Munch, H. Rudler, J.-C. Daran, C. Knobler and Y. Jeannin, *J. Organomet. Chem.*, *323* (1987) 371.

[18] (a) T.A. Mitsudo, H. Nakanishi, T. Inubushi, I. Morishima, Y. Watanabe and Y. Takegami, *J. Chem. Soc., Chem. Commun.*, (1976) 416; (b) W.A. Herrmann, J. Gimeno, J. Weichmann, M.L. Ziegler and B. Balbach, *J. Organomet. Chem.*, *213* (1981) C26; (c) T.A. Mitsudo, H. Watanabe, T. Sasaki, Y. Watanabe, Y. Takegami, H. Kafuku, K. Kinoshita and K. Nakatsu, *J. Chem. Soc., Chem. Commun.*, (1981) 22; (d) T.A. Mitsudo, Y. Ogino, Y. Komiya, H. Watanabe and Y. Watanabe, *Organometallics*, *2* (1983), 1202; (e) M.F. Semmelhack, R. Tamura, W. Schatter and J. Springer, *J. Am. Chem. Soc.*, *106* (1984) 5363.

[19] N. Walker and D. Stuart, *Acta Crystalllogr., A39* (1983) 158.

[20] A.C.T. North, D.C. Phillips and F.S. Mathews, *Acta Crystallogr.*, *A24* (1968) 351.

[21] D.J. Watkin, J.R. Carruthers and P.W. Betteridge, *CRYSTALS* User Guide, Chemical Crystallography Laboratory, University of Oxford, UK, 1985.

[22] G.M. Sheldrick, *SHELXS 86*, Program for Crystal Structure Solution, University of Gottingen, Gottingen, Germany, 1986.

[23] *International Tables for X-ray Crystallography,* Vol.IV, Kynoch, Birmingham, UK, 1974.